JOC Article

NMR Chemical Shifts. Substituted Acetylenes

Kenneth B. Wiberg,*[,1a] Jack D. Hammer,[1a] Kurt W. Zilm,*[,1a] Todd A. Keith,[1b] James R. Cheeseman,[1b] and James C. Duchamp[1c]

Department of Chemistry, Yale University, New Haven, Connecticut 06520, and Lorentzian Inc., 140 Washington Ave., North Haven, Connecticut 06473

kenneth.wiberg@yale.edu

Received August 11, 2003

The MPW1PW91/6-311+G(2d,p) and MP2/6-311+G(2d,p) GIAO nuclear shieldings for a series of monosubstituted acetylenes have been calculated using the MP2/6-311G(2d,p) geometries. Axially symmetric substituents such as fluorine may lead to large changes in the isotropic shielding but have little effect on the tensor component (zz) about the C≡C bond axis. On the other hand, substituents such as vinyl and aldehyde groups lead to essentially no difference in the isotropic shielding but are calculated to give a large zz paramagnetic shift to the terminal carbon of the acetylene group, without having much effect on the inner carbon. The tensor components of the chemical shifts for trimethylsilylacetylene, methoxyacetylene, and propiolaldehyde have been measured and are in reasonable agreement with the calculations. The downfield shift at the terminal carbon of propiolaldehyde along with a small upfield shift at the adjacent carbon has been found to result from the coupling of the in-plane π MO of the acetylene with the π^* orbital that has a node near the central carbon. The tensor components for acetonitrile also have been measured, and the shielding of cyano and acetylenic carbons are compared.

1. Introduction

NMR spectroscopy has become one of the major structural tools in chemistry. Although it is now possible to calculate the ^{13}C NMR chemical shifts with satisfactory accuracy using methods such as IGLO,[2] GIAO,[3] and IGAIM,[4] there has not been similar progress in the interpretation of these shifts in terms of simple models. We have studied this problem using tools that we have recently developed.[5] This report is concerned with acetylene and with a group of substituted acetylenes.

These compounds are of interest because of their large upfield long axis tensor components that are close to the maximum diamagnetic shielding for carbon.[6] Substituents can lead to marked changes in chemical shifts, but calculations for fluoroacetylene in which the isotropic chemical shifts differ by 72 ppm found that the long axis (zz) tensor component changed by only 5 ppm.[7] On the other hand, with phenylacetylene, which has only a small difference in isotropic chemical shift, there is a large difference in the *z* component (93 ppm).[8] A particularly intriguing aspect of substituent effects in acetylenes is that the acetylenic carbon β to the substituent often experiences a much greater change in shielding than the substituted carbon itself.

To gain information on the origin of these differences, we have calculated the nuclear shieldings for a variety of substituted acetylenes. The shielding (σ) with respect to a bare carbon nucleus is related to the chemical shift (δ) by

$$\sigma = 186.4 - \delta$$

where 186.4 is the shielding for TMS.[9] We use this scale for convenience in comparing experimental δ values to computed σ values. Because it is well-known that most shielding computations have small systematic errors, we do not place much significance on the differences observed in absolute shielding values arising in different calculation methods. A computational study concerned with absolute accuracy would recompute the TMS reference at each level of theory, as well as involve vibrational corrections. Ways of dealing with such comparisons have been discussed in some depth in the literature.[10] Our focus here, however, is on the physical origins of the shielding phenomena observed and calculated, not the absolute accuracy, and as such not central to our conclusions insofar as they are smaller than the effects to be discussed.

(1) (a) Yale University. (b) Lorentzian, Inc. (c) Emory and Henry College, P.O. Box 947, Emory, VA 24327.

(2) Schindler, M.; Kutzelnigg, W. *J. Chem. Phys.* **1982**, *76*, 1919; *J. Am. Chem. Soc.* **1983**, *105*, 1360; *Mol. Phys.* **1983**, *48*, 781.

(3) (a) Ditchfield, R. *Mol. Phys.* **1974**, *27*, 789. (b) Wolinski, K.; Hinton, J. F.; Pulay, P. *J. Am. Chem. Soc.* **1990**, *112*, 8251. (c) Compare Cheeseman, J. R.; Trucks, G. W.; Keith, T. A.; Frisch, M. J. *J. Chem. Phys.* **1996**, *104*, 5497 for the implementation that is found in Gaussian 94.

(4) Keith, T. A.; Bader, R. F. W. *Chem. Phys. Lett.* **1993**, *210*, 223.

(5) Compare Wiberg, K. B.; Hammer, J.; Zilm, K. W.; Cheeseman, J.; Keith, T. *J. Phys. Chem.* **1998**, *A102*, 8766 for the method of obtaining the coupling with the virtual orbitals using IGAIM.

(6) The calculated shielding for C-4 is 285 ppm.

(7) Bohmann, J.; Farrar, T. C. *J. Phys. Chem.* **1996**, *100*, 2646.

(8) Farrar, T. C.; Jablonsky, M. J.; Schwartz, J. L. *J. Phys. Chem.* **1994**, *98*, 4780.

(9) Jameson, A. K.; Jameson, C. J. *Chem. Phys. Lett.* **1987**, *134*, 461. Raynes, W. T.; McVay, R.; Wright, S. *J. Chem. Soc., Faraday Trans. 2* **1989**, *85*, 759.

(10) Auer, A. A.; Gauss, J.; Stanton, J. F. *J. Chem. Phys.* **2003**, *118*, 10407.

10.1021/jo030258i CCC: $27.50
Published on Web 01/16/2004

The geometries of the acetylenes were calculated at the MP2/6-311G(2d,p) theoretical level.[11] It is relatively difficult to reproduce the structures of acetylene and propyne.[12] MP2 calculations using a small basis set such as 6-31G* gives a C−C bond length that is too long (1.216 vs exptl 1.203). The MP2/6-311G(2d,p) basis set gives 1.2095 and the much larger aug-cc-pVTZ basis set gives 1.2092. Thus, 6-311G(2d,p) was chosen for all of the geometry optimizations.

The set of compounds includes unstable compounds such as hydroxyacetylene and aminoacetylene to provide a bridge between propyne and fluoroacetylene. Since some of these compounds have conjugated systems and lone pairs, it seemed advisable to correct for electron correlation and to include diffuse functions in the basis set. Therefore, the ^{13}C shieldings were calculated at the MPW1P91/6-311+G(2d,p) level. This basis set has been found to be suitable for the calculation of the nuclear shielding,[13] and additional polarization functions were found to have little effect on the calculated values. The MPW1P91 density functional model[14] was chosen because we have found it to better reproduce experimental data than other density functional models that were examined.[15] It also has an advantage over MP2 because it leads to wave functions in a compact form (i.e., all orbitals have an occupancy of either 2 or 0), which facilitates the analysis of the shielding in terms of the molecular orbitals.

Two theoretical models were used. In GIAO, the nuclear shielding is calculated as the second derivative of the energy with respect to the applied field and the nuclear moment using field dependent orbitals.[3] The IGAIM method first calculates the current density and then obtains the shielding density as the cross product of the current density and a vector from the nucleus in question, divided by the distance cubed. Integration of the shielding density gives the nuclear shielding.[4] The calculations were carried out using Gaussian 95.[16] These two quite different methods give essentially the same nuclear shielding using the above basis set. A comparison of the IGAIM and GIAO values is available as Supporting Information. The experimental chemical shifts with respect to TMS were converted to shielding as indicated above.

The MP2/GIAO[17] model also was used in order to allow a comparison with the DFT calculations. In most cases, the 6-311+G(2d,p) basis set was used, but for the larger molecules having six or more non-hydrogen atoms, it was necessary to use the 6-311G(d,p) basis set. With other compounds in this series, the change in basis set caused only 1−2 ppm changes in calculated shielding.

TABLE 1. Calculated and Observed Shielding for Acetylene and Propyne, 6-311+G(2d,p) Basis Set

			shielding, ppm			
compound	atom	axis	HF	MPW1PW91	MP2	obsd[a]
acetylene	C	*x*,*y*	36	29	50	36
		z	279	279	279	276
		iso	117	112	126	116 (110)
propyne	Ca	*x*,*y*	15	8	30	20
		z	299	293	284	279
		iso	110	103	115	106 (101)
	Cb	*x*,*y*	48	42	60	46
		z	258	261	273	260
		iso	118	115	131	117 (113)
	C(Me)	*x*,*y*	185	175	186	
		z	202	200	208	
		iso	191	184	194	(179)

[a] Solid-state spectra (ref 25). Values in parentheses are from solution spectra.

The isotropic shielding and the tensor components of the shielding for acetylene and propyne have been measured[18] and are compared with the calculated shielding in Table 1. The agreement between the calculated and observed isotropic shielding for acetylene is quite good for both MPW1PW91 and MP2. The *z* component of the shielding for acetylene is 279 ppm at all theoretical levels, and it agrees with the experimental value within its estimated uncertainty. This corresponds to just diamagnetic shielding. As we have found in many other cases, the DFT shielding for the *x* and *y* axes is less than the HF shielding, whereas the MP2 shielding is greater. These differences are at the level of the systematic shielding differences between these two methods, and therefore in and of themselves not physically significant.

Propyne also has been studied experimentally, and again, the MPW1PW91 calculated isotropic shielding are in good agreement with the experimental values. With the β carbon, the DFT calculated shielding is in very good agreement with experiment, but for the α carbon, the MP2 shielding is in better agreement with experiment. It should be noted that the calculations are for the gas phase, whereas the measurements are made for the solid phase and have an uncertainty of about ±5 ppm. It is known that the phase affects the magnitude of the chemical shifts.[19]

2. Acetylene

Since acetylene is a linear molecule, it will not have paramagnetic shielding about the *z* axis.[20] It is strongly diamagnetically shielded about this axis, leading to a large upfield chemical shift (Table 1). The *z* axis shielding

(11) Hehre, W. J.; Radom, L.; Schleyer, P. v. R.; Pople, J. A. *Ab Initio Molecular Orbital Theory*; Wiley: New York, 1986.

(12) The observed structures are acetylene, C≡C = 1.203(1) Å (Berry, R. J.; Harmony, M. D. *Struct. Chem.* **1990**, *1*, 49); propyne, C≡C = 1.204(1) Å, C−C = 1.458 Å (LeGuennec, M.; Demaison, J.; Wlodarczak, G.; Marsden, C. J. *J. Mol. Spectrosc.* **1993**, *160*, 471). The MP2/6-31G* structures had acetylene, C≡C = 1.216 Å, propyne, C≡C = 1.220 Å, C−C = 1.463 Å.

(13) Cheeseman, J. R.; Trucks, G. W.; Keith, T. A.; Frisch, M. J. *J. Chem. Phys.* **1996**,*104*, 5497.

(14) Adamo, C.; Barone, V. *Chem. Phys. Lett.* **1997**, *274*, 242. Perdew, J. P.; Burke, K.; Wang, Y. *Phys. Rev.* **1996**, *B54*, 16533.

(15) Wiberg, K. B. *J. Comput. Chem.* **1999**, *20*, 1299.

(16) Frisch, M. J.; Trucks, G. W.; Schlegel, H. B.; Gill, P. M. W.; Johnson, B. G.; Robb, M. A.; Cheeseman, J. R.; Keith, T.; Petersson, G. A.; Montgomery, J. A.; Raghavachari, K.; Al-Laham, M. A.; Zakrzewski, V. G.; Ortis, J. V.; Foresman, J. B.; Cioslowski, J.; Sefanov, B. B.; Nanayakkara, A.; Challacombe, M.; Peng, C. Y.; Ayala, P. Y.; Chen, W.; Wong, M. W.; Andres, J. L.; Replogle, E. S.; Gomperts, R.; Martin, R. L.; Fox, D. J.; Binkley, J. S.; Defrees, D. J.; Baker, J.; Stewart, J. P.; Head-Gordon, M.; Gonzalez, C.; Pople, J. A. *Gaussian 95*, Development Version (Rev. D); Gaussian, Inc.: Pittsburgh, PA, 1995.

(17) Gauss, J.; Stanton, J. F. *Chem. Phys. Lett.* **1992**, *191*, 614. Gauss, J.; Stanton, J. F. *J. Chem. Phys.* **1993**, *99*, 3629.

(18) Zilm, K. W.; Grant, D. M. *J. Am. Chem. Soc.* **1981**, *103*, 2913. Beeler, A. J.; Ordendt, A. M.; Grant, D. M.; Cutts, P., W.; Michl, J.; Zilm, K. W.; Downing, J. W.; Facelli, J. C.; Schindler, M. S.; Kutzelnigg, W. *J. Am. Chem. Soc.* **1984**, *106*, 7672.

(19) Compare Webb, G. A. In *Nuclear-Magnetic Shieldings and Molecular Structure*; Tossell, J. A., Ed.; Kluwer Academic Publishers: The Netherlands, 1993; p 16.

(20) Ramsey, N. F. *Phys. Rev.* **1950**, *78*, 699.

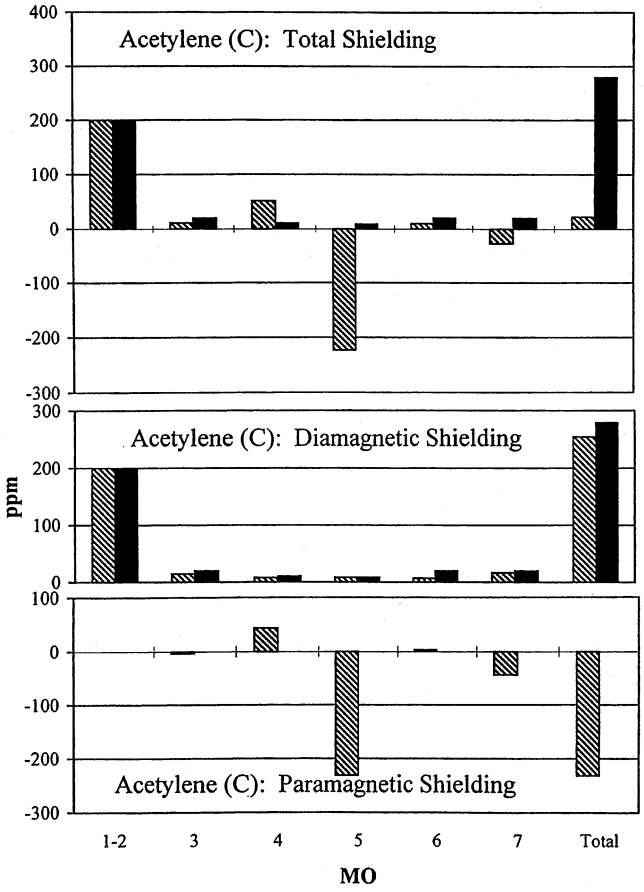

FIGURE 1. Shielding components for acetylene. The solid bars refer to the *z* axis, and the hashed bars refer to the *x* and *y* axes.

is close to the maximum diamagnetic shielding for carbon and is derived in part from the current density associated with the pair of degenerate π orbitals. The shielding for the *x* and *y* axes is relatively weak.

The smaller shielding for the *x* and *y* axes results from a paramagnetic term that opposes the diamagnetic shielding. To further study the deshielding about these axes, the tensor components were calculated on an MO basis using IGAIM (Figure 1).[5] In this procedure, the nucleus in question is used as the gauge origin. The division between diamagnetic and paramagnetic components is gauge-dependent, but this appears to be a logical choice, especially since the 1s electrons, which can only give diamagnetic shielding, are properly represented using this gauge origin. The two linear combinations of the carbon 1s orbitals (MO 1 and 2) give a large diamagnetic shift of about 200 ppm. Small diamagnetic contributions are found for several of the other orbitals, and the paramagnetic *x* and *y* axis shifts are clearly derived from MO 5. A paramagnetic shift results from mixing an occupied MO with one or more of the virtual MOs in the presence of a magnetic field. The important virtual MOs may be found using the IGAIM method[5] and are summarized in Table 2.

MO 5 and the important virtual MOs are shown in Figure 2. MO 5 is a σ orbital formed from p_z atomic orbitals (where *z* is the long axis). The virtual MO 9 is a π^* orbital formed from p_y ao's, and MO 16 is similar but with an additional node. In the presence of a magnetic field in the *x* direction, the angular momentum operator will rotate the p_z ao's in MO 5 so that they can mix with the p_y ao's in the virtual orbitals, leading to a downfield paramagnetic shift. This provides a simple explanation for the differences in the tensor components for acetylene.

TABLE 2. Shielding Components Derived from MO 5 of Acetylene

virtual MO	σ_{xx}
9	−105.5
16	−44.2
28	−25.9
36	−10.7
42	−4.6
55	−9.9
75	−0.8
sum	−201.6
total[a]	−219.0

[a] Includes all of the virtual MOs.

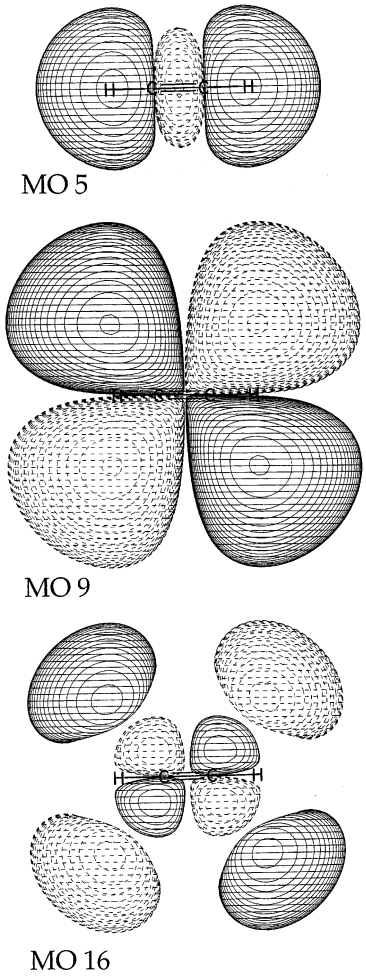

FIGURE 2. Occupied MO 5 and virtual MOs 9 and 16 of acetylene.

3. Axially Symmetrical Substituted Acetylenes

The isotropic shieldings for a series of axially symmetrical substituted acetylenes were calculated and are compared with the available experimental data in Table 3. Once more, the systematic trend of the MP2 shieldings to be about 10 ppm larger than the DFT calculated values

TABLE 3. Calculated Nuclear Shielding of Axially Symmetrical Substituted Acetylenes

	MPW1PW91		MP2		obsd	
compound	β	α	β	α	β	α
	Shielding					
HC≡CH	112	112	126	126	116	116
HC≡CCH$_3$	103	115	115	131	106	117
HC≡CF	92	173	101	185	102	177
HC≡CSiH$_3$	105	82	116	104		
HC≡CSiMe$_3$	94	87	109	109	96	93
HC≡CCl	117	127	129	141		
HC≡CNH$_3^+$	130	111	137	130		
HC≡C−NMe$_3^+$	110	116	122	119		
HC≡CCN	122	113	135	129	129	112
HC≡C−C≡CH	114	120	126	134	120	120[a]
FC≡CF	134	134	142	142		
FC≡C−C≡CF	98	173	107	184		
NC−C≡C−C≡C−CN	130	130	140	140		
	Shift Relative to Acetylene (+ Indicates Deshielding)					
HC≡CCH$_3$	9	−3	11	−5	6	−1
HC≡CF	20	−61	25	−69	14	−61
HC≡CSiH$_3$	7	30	10	22		
HC≡CSiMe$_3$	18	25	17	17	20	23
HC≡CCl	−5	−15	−3	−15		
HC≡CNH$_3^+$	−18	1	−11	−4		
HC≡C−NMe$_3^+$	2	−4	4	7		
HC≡CCN	−10	−1	−9	−3	−13	4
HC≡C−C≡CH	−2	−8	0	−6	−4	−4
FC≡CF	−22	−22	−16	−16		
FC≡C−C≡CF	14	−61	19	−53		
NC−C≡C−C≡C−CN	−18	−18	−14	−14		

[a] Average of α and β carbons.

is likely a referencing issue. The quantity of major interest is the change in shielding with respect to acetylene, and these data for MPW1PW91/GIAO and MP2/GIAO are given in Table 3. It is encouraging to find that the shifts relative to acetylene as expected are essentially the same for the two procedures and that they agree with the experimental relative shieldings. The components of the nuclear shielding are summarized in Table 4.

Some substituents lead to significant changes in shielding. Fluorine leads to one of the larger effects at both C_α and C_β, and we have previously examined it in connection with its ^{19}F chemical shift.[21] Some of the previous analysis will be repeated in order to provide a context for examining the other compounds.

Both the total shielding and the paramagnetic components for fluoroacetylene have been calculated on an MO basis, giving the data recorded in Figure 3. In comparing this compound with acetylene, it is convenient to correlate its MOs with those of acetylene, and this is shown in Table 5.

It can be seen that the largest paramagnetic term is derived from MO 7, which is related to MO 5 of acetylene. Thus, this type of orbital gives the main *x* and *y* paramagnetic components for both compounds. However, the difference in magnitude for the two carbons is negligible and contributes little to the difference in chemical shift between these carbons.

The main contribution to the difference is the degenerate pair of π MOs, 10 and 11, with a smaller contribution from the other pair of π MOs, 8 and 9. MO 6 also contributes to the difference. These MOs are shown in Figure 4. The major contribution from MO 10 arises from an interaction with virtual MO 12. The nature of MO 12 is not easily appreciated from the MO plot (Figure 4) because of the considerable contribution from 2s orbitals that do not contribute to paramagnetic shielding. The p-orbital contributions to this MO at C_α and C_β are shown in Figure 5. The component at C_α will interact with MO 10 in the presence of a magnetic field to give a large paramagnetic term. The component at C_β after rotation will have little overlap with MO 10 and will give a negligible paramagnetic term. The difference between C_α and C_β in MO 12 results from the high electronegativity of the fluorine.

(21) Wiberg, K. B.; Hammer, J. D.; Zilm, K. W.; Cheeseman, J. R.; Keith, T. A. *J. Phys. Chem. A* **1998**, *102*, 8766.

TABLE 4. Calculated Components of Nuclear Shielding of Axially Symmetric Substituted Acetylenes

		MPW1PW91		MP2	
compound	atom	*xx,yy*	zz	*xx,yy*	zz
HC≡CH	C	29	279	50	279
HC≡CCH$_3$	Cα	8	293	30	284
	Cβ	42	261	60	273
HC≡CF	Cα	−5	287	8	287
	Cβ	119	281	136	281
HC≡CSiH$_3$	Cα	12	290	36	276
	Cβ	−2	250	21	270
HC≡CSiMe$_3$	Cα	−5	293		
	Cβ	8	245		
HC≡CCl	Cα	30	290	48	290
	Cβ	49	282	70	282
HC≡CNH$_3^+$	Cα	50	292	64	284
	Cβ	35	262	58	273
HC≡C−NMe$_3^+$	Cα	14	301	27	314
	Cβ	55	239	60	230
HC≡CCN	Cα	40	287	58	287
	Cβ	30	280	53	280
	CN	−34	286	−9	297
HC≡C−C≡CH	Cα	28	287	45	287
	Cβ	40	281	60	281
FC≡CF	C	57	288	70	282
FC≡C−C≡CF	Cα	4	288	16	288
	Cβ	115	290	131	290
NC−C≡C−C≡C−CN	Cα	52	287	66	287
	Cβ	−35	287	−9	297
CH$_3$CN	CN	−51	291	−23	281

4. Experimental Study of Trimethylsilylacetylene and Methoxyacetylene

Before proceeding further, it seemed appropriate to obtain additional experimental data in order to have a comparison with the calculated tensor components. We have chosen to study trimethylsilylacetylene, in which an electron-releasing group is attached to the acetylene, and methoxyacetylene, in which an electron-withdrawing methoxy group is attached. The calculations for the latter (cf. the next section) indicate that it is similar to fluoroacetylene.

The powder pattern spectrum for trimethylsilylacetylene is given in Figure 6. The peak at 140 ppm is a quadrature image of the methyl peak that results from the real and imaginary channels having different amounts of amplification. Although it was not present in any of the other spectra for this compound obtained subsequently, the relevant features of these spectra are not as clear as those in Figure 6. The small wiggle at ~65 ppm is due to the carrier frequency.

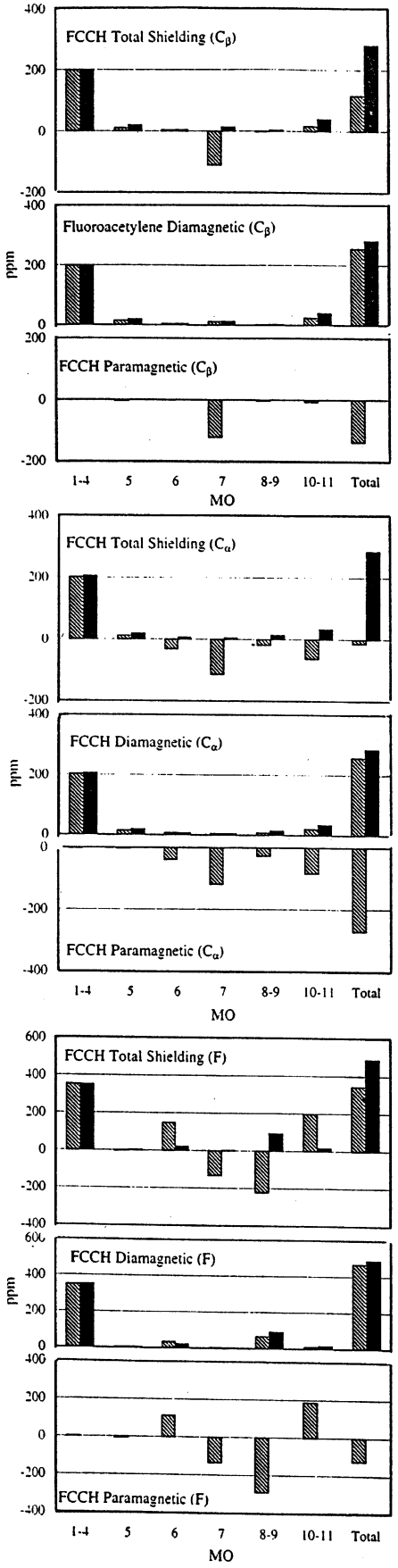

FIGURE 3. Shielding components for fluoroacetylene. The solid bars refer to the *z* axis, and the hashed bars refer to the *x* and *y* axes.

TABLE 5. Correlation of Acetylene and Fluoroacetylene MOs

acetylene		fluoroacetylene	
		1	F1s
1	C1s	2	C1s
2	C1s	3	C1s
		4	F2s
3	C1(2sp) + C2(2sp) + H's	5	C1(2sp) + C2(2sp) + H's + F(2p)
4	C1(2sp) − C2(2sp) + H's	6	C1(2sp) − C2(2sp) + H's − F(2p)
5	C−C bonding	7	C−C bonding
6	π	8	π, all bonding
7	π	9	π, all bonding
		10	π', C−C bonding, F antibonding
		11	π', C−C bonding, F antibonding
		12	σ antibonding
		13	σ antibonding
8	π^*	14	π^*
9	π^*	15	π^*
		16	$\pi^{*\prime}$
		17	$\pi^{*\prime}$

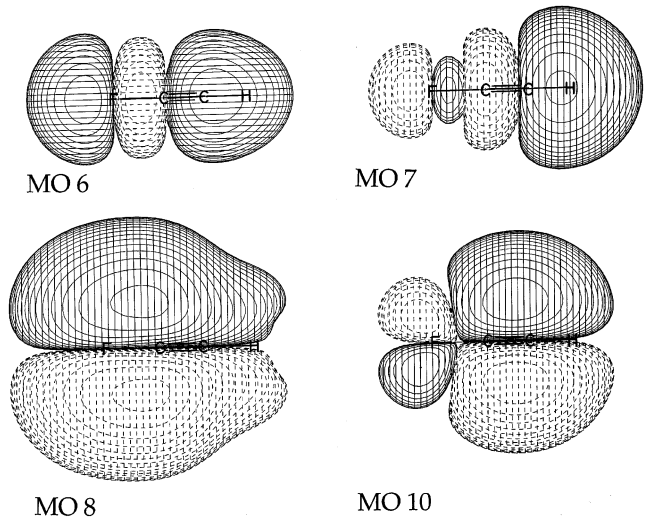

FIGURE 4. Occupied MOs 6, 7, 8, and 10 of fluoroacetylene. MOs 9 and 11 correspond to 8 and 10, but rotated about the *z* axis by 90°.

The two bands at the left side of the spectrum (indicated with arrows) correspond to the $\sigma_\perp$ tensor components of the two acetylene carbons, while the two shoulders at the right-hand side of the spectrum correspond to the $\sigma_{||}$ components. The shoulder at ca. −50 ppm, corresponding to the $\sigma_{||}$ component of the β carbon, is not well resolved and was calculated on the basis of the experimentally measured $\sigma_\perp$ and isotropic shift values obtained from magic angle spinning experiments (Table 6).

Because the $\sigma_\perp$ values are very similar for the two acetylenic carbons, a dipolar-dephasing[22] experiment was performed to help clarify the assignment. Since only the β carbon is attached to a proton, the dipolar-dephased spectrum should result in a diminished C_β intensity relative to that of C_α. The dephased spectrum shows that the right-hand band has been attenuated, which suggests

(22) Opella, S. J.; Frey, M. H. *J. Am. Chem. Soc.* **1979**, *101*, 5854.

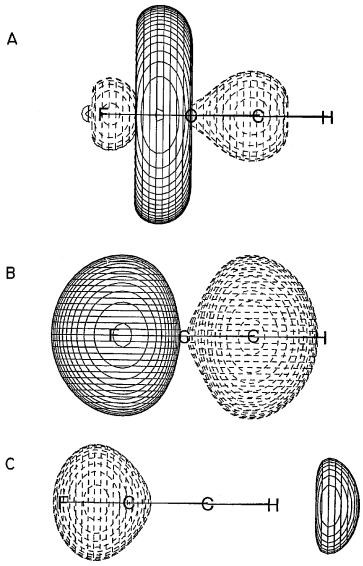

FIGURE 5. (A) MO 12 of fluoroacetylene. (B) The p-AO component at C_α'. (C). The π-AO component at C_β.

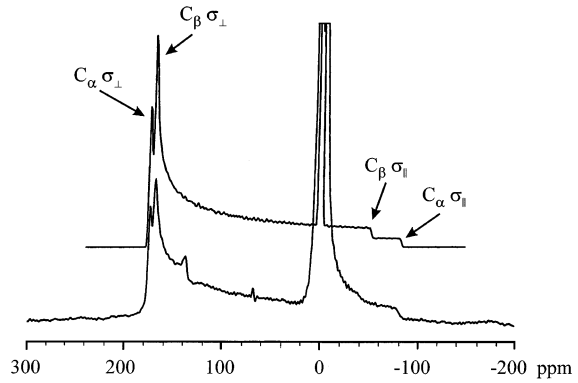

FIGURE 6. Solid-state ^{13}C NMR spectrum of trimethylsilylacetylene. The calculated spectrum is given above the experimental spectrum.

that the $\sigma_\perp$ component for C_α is downfield from that of C_β, in agreement with the computational results.

In methoxyacetylene, only the tensor components for C_α could be obtained unambiguously (Figure 7). Two spectra, obtained using different probes, were different in the central parts, suggesting that torsional motion of the methyl group about the acetylene bond axis was still present even at the lowest temperatures accessible using these probes (−170 °C). However, the shoulder at 94 and the band at 68 ppm are found in all of the spectra and may tentatively be assigned as δ_{11} and δ_{22} for C_β. This would be in accord with the calculated spectrum (not shown).

The results of these experiments are summarized in Table 6. The calculations for methoxyacetylene indicate that the substituent effect is similar to that in fluoroacetylene. In both compounds, the effect produces a large difference between the isotropic shifts for C_α and C_β. With respect to acetylene, neither substituent changes the shielding when the field is applied along the acetylene bond. However, both substituents induce large shifts (in opposite directions for the two carbons) when a field is applied perpendicular to the acetylenic bond. Thus, it is

TABLE 6. Experimental and Computed Chemical Shift Tensor Components

	δ_{11}	δ_{22}	δ_{33}	δ_{MAS}	δ_{soln}
Experimental					
1. trimethylsilylacetylene					
Cα	176	176	−79	91	90
C*β*	171	171	−48	98	93
2. methoxyacetylene					
Cα	183	179	−84	93	92
C*β*	94	68	−78	28	26
3. propiolaldehyde					
Cα	161	161	−82	80	82
C*β*	142	130	−5	88	83
CHO	270	200	75	183	177
4. acetonitrile					
CN	224	224	−84	120	116
Me	9	9	−5	4	2
Calculated Chemical Shifts					
1. trimethylsilylacetylene					
Cα	191	191	−107	82	
C*β*	178	178	−59	99	
2. methoxyacetylene					
Cα	195	193	−105	94	
C*β*	89	69	−105	26	
3. propiolaldehyde					
Cα	183	176	−105	85	
C*β*	141	135	−14	88	
4. acetonitrile					
Cα	237	237	−105	123	
Me	9	9	−15	1	

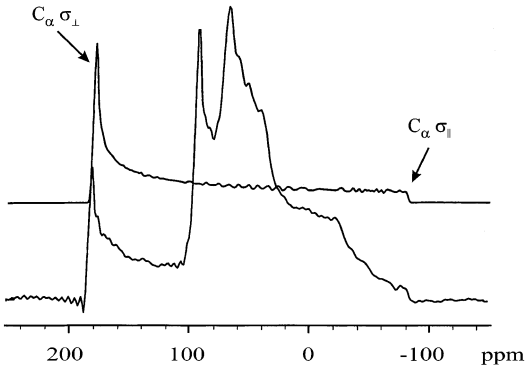

FIGURE 7. Solid-state ^{13}C NMR spectrum of methoxyacetylene. The calculated spectrum for C_α is given above the experimental spectrum.

the perpendicular shielding components that lead to the large differences in the isotropic shifts.

5. Substituents with a Plane of Symmetry

In contrast to the substituents given above, other substituents such as CHO, CH=CH_2, and NO_2 will break the degeneracy of the acetylene π-MOs. The shieldings for a number of acetylenes bearing groups of this type were calculated, giving the data in Table 7. The DFT method gives quite good agreement between calculated and experimental shieldings, but MP2 is significantly less successful. The relative chemical shifts vs acetylene are also given in Table 7 and here both methods give satisfactory results for methoxyacetylene, but whereas MPW1PW91 gives very good agreement with experiment for vinylacetylene, phenylacetylene, and propiolaldehyde, the MP2 results are much less satisfactory. It may be noted that the latter method gives differences in shielding

TABLE 7. Calculated Isotropic Shieldings for Substituted Acetylenes with a Plane of Symmetry

	MPW1PW91		MP2		obsd	
compound	α	*β*	α	*β*	α	*β*
Shielding						
aminoacetylene	102	138	111	154		
hydroxyacetylene	96	162	105	174		
methoxyacetylene	92	160	101	173	94	160
acetylenethiol	115	102	125	124		
thiomethoxyacetylene	105	100	124	114		
nitroacetylene	102	128	101	161		
vinylacetylene	100	101	128	106	103	106
phenylacetylene	99	101	106	130	103	109
propiolaldehyde	98	101	132	102	104	103
Shielding vs Acetylene (+ Indicates Deshielding)						
aminoacetylene	10	−26	15	−28		
hydroxyacetylene	16	−50	21	−48		
methoxyacetylene	20	−48	25	−47	22	−44
acetylenethiol	−3	10	1	2		
thiomethoxyacetylene	7	12	2	12		
nitroacetylene	10	−16	25	−35		
vinylacetylene	12	11	−2	20	13	10
phenylacetylene	13	11	20	−4	13	10
propiolaldehyde	14	11	6	24	12	13

TABLE 8. Calculated Shielding Components for Substituted Acetylenes with a Plane of Symmetry

		MPW1PW91			MP2		
compound	atom	*xx*	*yy*	*zz*	*xx*	*yy*	*zz*
acetylene	C	29	29	279	50	50	279
fluoroacetylene	Cα	−5	−5	287	8	8	287
	C*β*	119	119	281	136	136	281
aminoacetylene	Cα	−6	21	291	125	35	284
	C*β*	59	106	248	80	117	267
hydroxyacetylene	Cα	−7	6	289	9	20	287
	C*β*	94	120	271	112	133	277
methoxyacetylene	Cα	−9	−7	291	6	7	289
	C*β*	97	117	266	115	132	273
acetylenethiol	Cα	12	46	304	41	61	271
	C*β*	15	45	246	38	56	282
thiomethoxyacetylene	Cα	1	18	295	29	33	280
	C*β*	23	48	229	49	63	261
nitroacetylene	Cα	5	13	288	17	32	256
	C*β*	90	69	224	105	92	285
vinylacetylene	Cα	2	3	299	23	23	271
	C*β*	44	52	204	62	70	251
phenylacetylene	Cα	−8	6	298	17	31	271
	C*β*	43	54	207	65	72	253
propiolaldehyde	Cα	3	10	291	24	24	259
	C*β*	45	51	200	66	68	261

between the α and *β* carbons of the above compounds of 20−30 ppm, whereas both the DFT calculations and experiments give a much smaller difference. One however must be cautious in interpreting these differences as indicators of the ultimate accuracy of the calculations as vibrational corrections have not been applied here.[10]

It was noted above that a fluorine substituent leads to shielding at the *β* carbon and deshielding at the α carbon. It can be seen in Table 8 that NH_2, OH, and OMe also lead to this change in shielding. Fluorine gives the largest effect, OH and OMe give a smaller effect, and NH_2 gives the smallest difference. This is clearly an electronegativity effect and is associated with changes in the *σ** orbital. It might also be noted that similar changes are seen in the *z*-axis tensor components for these compounds. Here, an occupied *π* orbital (MO 11) couples with the *π** orbital (MO 14) in a perpendicular plane (Figure 8). Since *π** has the opposite phase for the p orbitals as compared to *π*, one carbon will experience a deshielding paramagnetic interaction, whereas the other will experience a shielding paramagnetic interaction.[5]

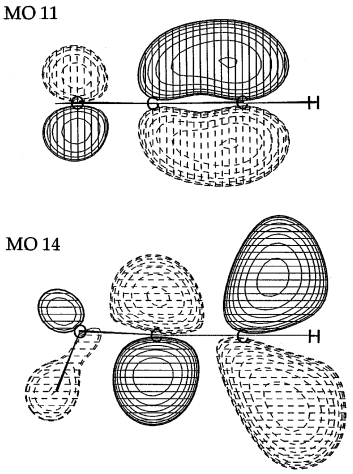

FIGURE 8. The *π* and *π** MOs of methoxyacetylene that lie in perpendicular planes.

Unlike the axially symmetrical substituents, the planar substituents sometimes lead to large differences in the *zz* components of the shift (Table 8). With the oxygen-containing groups, the differences are relatively small, but with groups such as vinyl, phenyl, or carboxaldehyde, the difference in the *zz* components approaches 100 ppm for the DFT calculations but remains relatively small for the MP2 calculations.

6. Vinylacetylene, Phenylacetylene, and Propiolaldehyde

The results for vinylacetylene, phenylacetylene, and propiolaldehyde (HC≡CCHO) are particularly interesting. Here, the DFT calculated isotropic shifts for the acetylenic carbons are about the same, in accord with the experimental data. However, the *z* tensor components are markedly different, and the *x* and *y* components change so as to compensate for the difference in *z*. The MP2 results are quite the opposite, with only a small difference in the *z* components. With vinylacetylene and the aldehyde, MP2 gives only a small difference between the *x* and *y* components of the shielding, whereas they are larger for DFT. The DFT results agree with the expectation that conjugation of one of the acetylenic *π* orbitals with another double bond will break the *π*-symmetry of the triple bond, whereas the MP2 results suggest that such an interaction is not important with these compounds.

The only experimental data previously available for the shielding anisotropy of these compounds is for the *β*-position of phenylacetylene where it was found to be 159 ± 3 ppm.[8] This is given by $\sigma_{zz} - (\sigma_{yy} + \sigma_{zz})/2$; for the DFT calculation it is 159 ppm, whereas for the MP2 calculation it is 185 ppm. Clearly, the DFT calculation yields a result that is closer to agreement with the experimental data than does the MP2 calculation. In the following, we shall further analyze the DFT calculations.

An MO analysis of the DFT shielding components for propiolaldehyde is shown in Figure 9 for the four highest

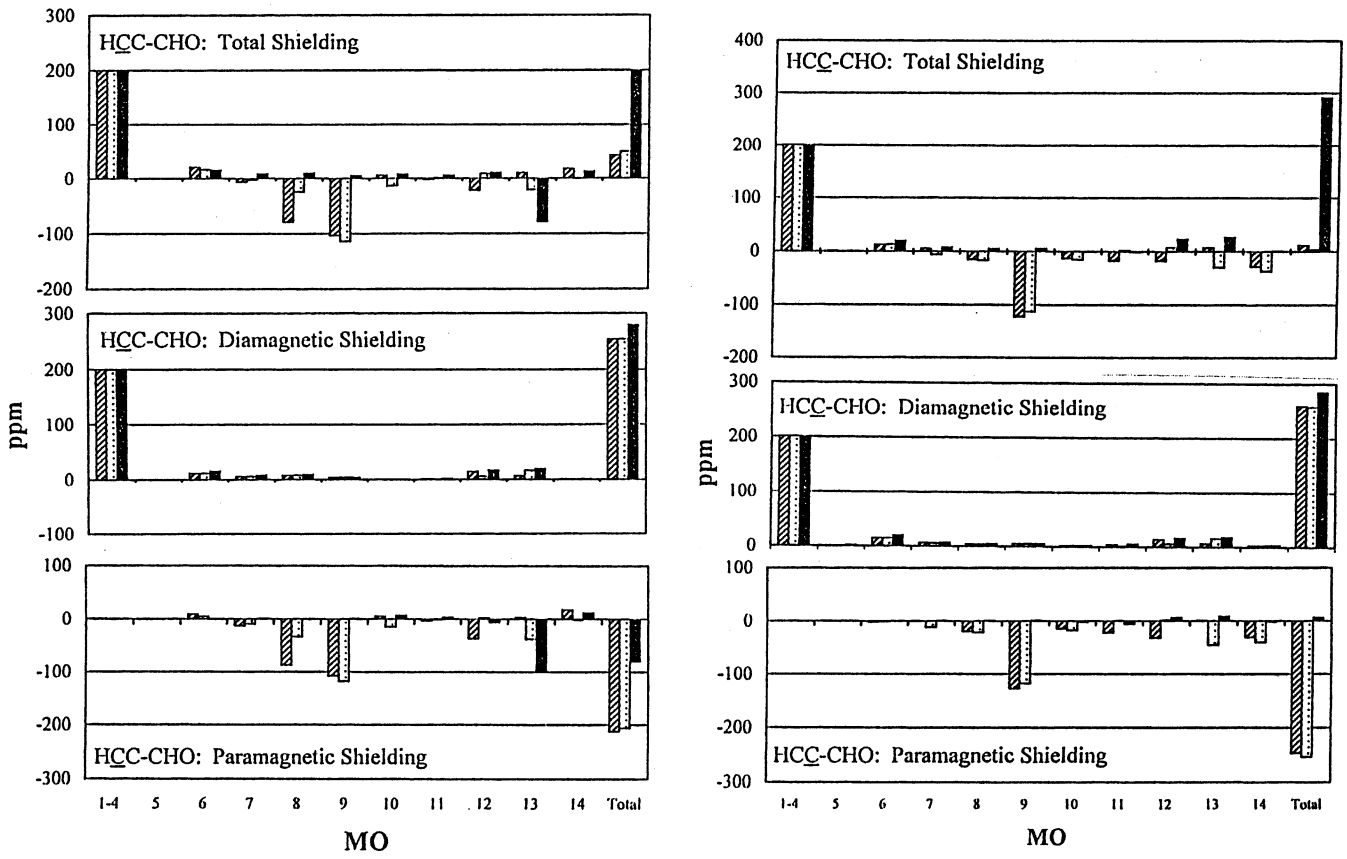

FIGURE 9. Shielding components for propiolaldehyde. The hashed bars refer to the *x* axis, the dotted bars refer to the *y* axis, and the solid bars refer to the *z* axis.

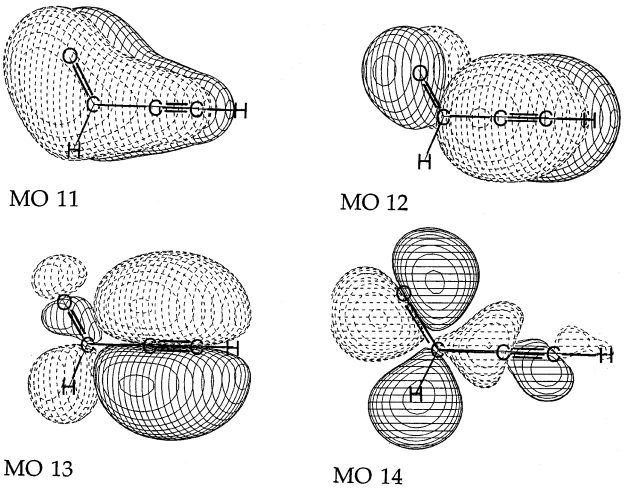

FIGURE 10. Four highest occupied MOs of propiolaldehyde.

occupied MOs of the aldehyde. There are no significant contributions to the shielding at C_α and C_β from the carbonyl group, and at each atom, the contribution from the adjacent atom is small. At C_α (the internal carbon), the *z* tensor components lead to an upfield (diamagnetic) shift. However, at C_β (the terminal carbon) the *z* component from MO 13 leads to a downfield (paramagnetic) shift. This component is the primary origin of the difference in the *z* tensor of the shielding at C_α and C_β.

The four highest occupied MOs are shown in Figure 10. MO 11 corresponds to the positive linear combination

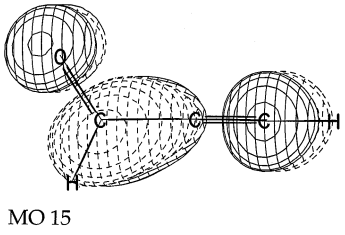

FIGURE 11. Virtual MO 15 of propiolaldehyde.

of the C=O and out-of-plane C≡C π-orbital, and MO 12 is the negative linear combination. MO 13 is the in-plane C≡C π-orbital. MO 14 involves the oxygen lone pairs and has largely σ character for the C≡C bond. The paramagnetic shift derived from MO 13 must involve an orthogonal π^* orbital since it arises from the angular momentum operator coupling an occupied MO with an orthogonal virtual MO. An examination of the matrix elements between the occupied and virtual orbitals showed that it arose from the lowest virtual orbital, MO15 (Figure 11), and that no other virtual orbitals contributed significantly. It is unique in that it has a node close to C_α, and as a result C_α is not much affected when the angular momentum operator couples MO 13 and MO 15. C_β, on the other hand, is strongly affected.

To be sure that this analysis is general, it also was applied to vinylacetylene. The IGAIM analysis is shown in Figure 12. Here both MO 13 and MO 14 (Figure 13) lead to downfield shifts in the *z* direction at C_β. The contribution from MO 13 is the larger term, and an

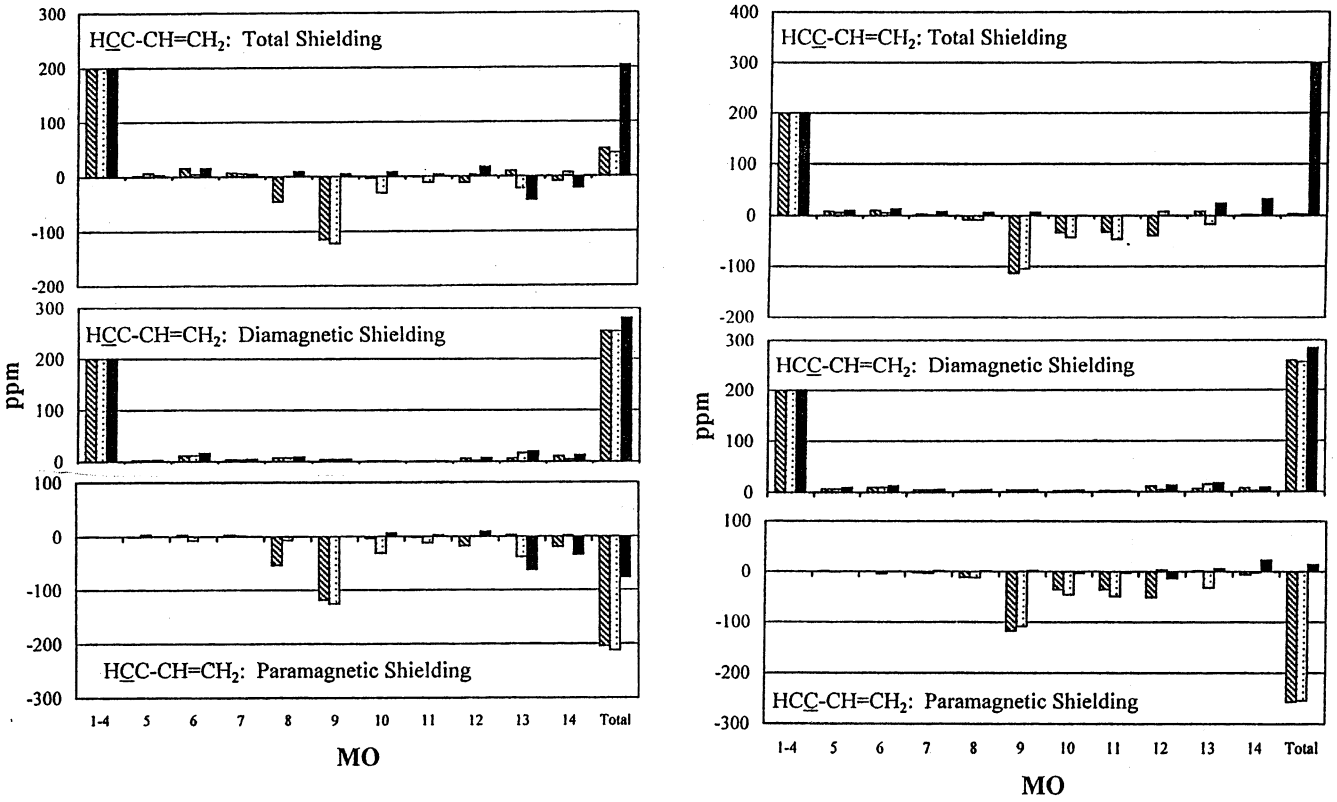

FIGURE 12. Shielding components for vinylacetylene. The hashed bars refer to the *x* axis, the dotted bars refer to the *y* axis, and the solid bars refer to the *z* axis.

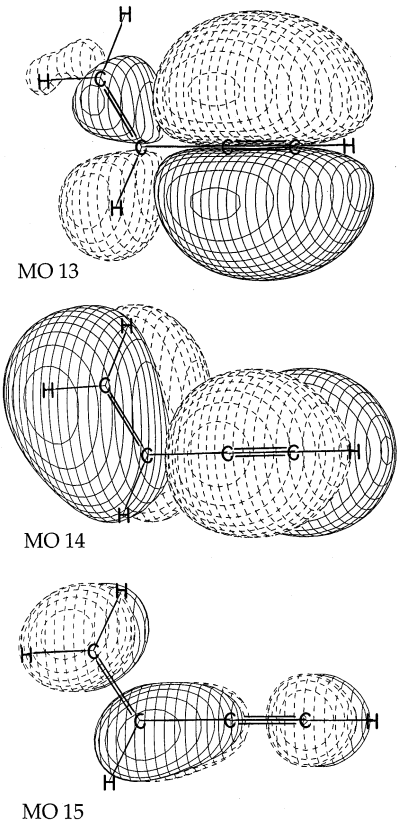

FIGURE 13. Occupied MOs 13 and 14 and virtual MO 15 of vinylacetylene.

examination of the coupling coefficients indicates that the only significant coupling is to MO 15 (Figure 13). Again,

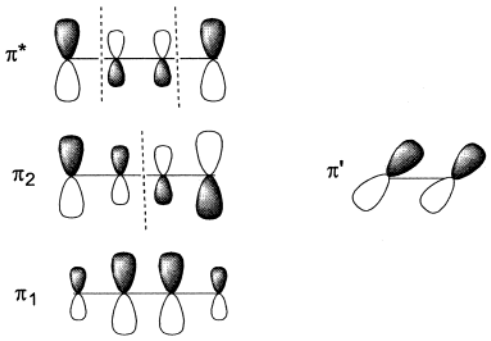

FIGURE 14. Hückel π-MOs for vinylacetylene.

the node is close to C_α, and no significant paramagnetic contribution would be expected at this atom, in contrast to C_β for which there is a large coefficient in MO 15. MO 14 is weakly coupled to many of the virtual orbitals, and it is therefore more difficult to analyze the origin of the downfield shift from this MO.

Why should the node in MO 15 for both propiolaldehyde and vinylacetylene be close to C_α? A simple Hückel representation of the π MOs is shown in Figure 14. The double bond p orbitals and the corresponding triple bond orbitals form a butadiene-like set of MOs, the first two of which are filled. The other set of triple bond p orbitals form a filled orthogonal π-MO, corresponding to MO 13. In the π^* MO (that corresponds to MO 15), one of the nodes will come close to C_α, and at a minimum, there will be a larger paramagnetic shift at C_β than at C_α. In addition, the phase of the p orbital at C_α is opposite to that at C_β. As a result, the paramagnetic deshielding at

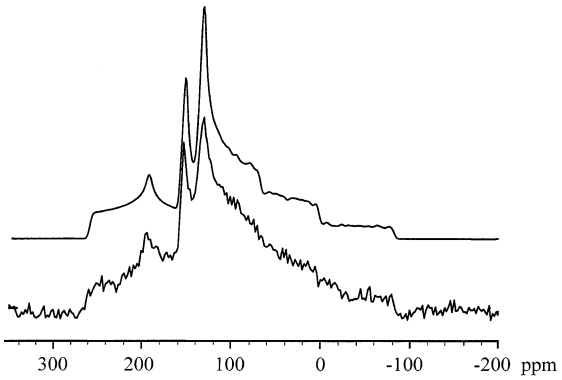

FIGURE 15. Solid-state ^{13}C NMR spectrum of propiolaldehyde. The calculated spectrum is given above the experimental spectrum.

TABLE 9. Experimental and Calculated Shift Tensor Components for Propiolaldehyde

			calculated	
atom	component	observed	B3LYP/GIAO	MP2/GIAO
C_β	*xx*	142	141	142
	yy	130	135	131
	zz	−5	−14	−12
	iso	88	88	87
C_α	*xx*	161	184	176
	yy	161	176	162
	zz	−82	−105	−131
	iso	80	85	69
CHO	*xx*	200	183	166
	yy	75	82	65
	zz	270	279	299
	iso	183	181	177

C_β will be accompanied by a small shielding paramagnetic term at C_α.

7. Experimental Measurements for Propiolaldehyde

It appeared desirable to study propiolaldehyde experimentally in order to check the accuracy of the ab initio calculations. The low-temperature solid-state NMR spectrum is shown in Figure 15. Several of the tensor components could readily be identified. To obtain additional data, the tensor components were derived from the relative intensities of the spinning sidebands in a slow magic angle spinning experiment for the same sample. Using different spinning speeds, it was possible to determine the isotropic shifts, since they are not sensitive to the spinning speed. The values thus obtained were 88, 73, and 180 ppm and corresponded to C_β, C_α, and the carbonyl carbon, respectively. Combining the powder pattern data with the isotropic shifts and a Herzfeld−Berger sideband analysis[23] gave the results shown in Table 9. It can be seen that the calculated shifts for C_β and CHO are in quite good agreement with the observed shifts, but those for C_2 have an error of about 20 ppm.

8. ^{13}C Chemical Shifts of Cyano Carbons

The cyano group is isoelectronic with an acetylene but has an electronegative atom attached to the carbon. It was of interest to examine the tensor components of the chemical shift of these carbons. Acetonitrile has been examined in an early solid-state study[24] and also has been examined using liquid crystalline media.[25] These studies have led to a range of values for the tensor components.

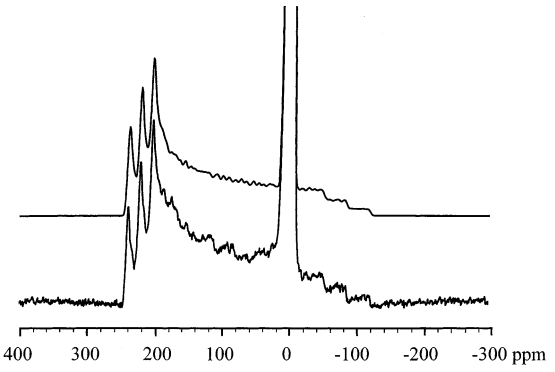

FIGURE 16. Solid-state ^{13}C NMR spectrum of acetonitrile. The calculated spectrum is given above the experimental spectrum.

TABLE 10. Chemical Shifts for Cyano Compounds Relative to TMS, B3LYP/6-311+G**

				isotropic	
compound	atom	*xx* = *yy*	*zz*	calcd	obsd[a]
acetonitrile	C(Me)	10.9	−13.9	2.6	0.3
	C(≡N)	240.5	−106.6	124.8	117.7
cyanogen	C(≡N)	210.7	−101.1	106.8	
dicyanoacetylene	C(≡C)	137.7	−103.0	57.5	
	C(≡N)	223.9	−102.3	115.2	

[a] Values observed in solution

We have reexamined the solid-state ^{13}C NMR spectrum of acetonitrile (Figure 16) The experimental shielding values are given in Table 6 and are in reasonably good agreement with the calculated values. The spectral features clearly show the dipolar coupling due to the ^{14}N (spin = 1), and the coupling constant was easily determined (R = 1300 Hz). The coupling constant is related to the internuclear distance between the two nuclei,[26] giving a C≡N bond length of 1.188 Å. This is 2.7% longer than the microwave value (1.157 Å[27]). However, it is known that rodlike molecules such as acetonitrile can have significant librational motion in the solid state.[26] This motion decreases the apparent dipolar coupling, which in turn leads to a small overestimation of the bond length. The librational motion also decreases the apparent shielding anisotropy, and this may account for the smaller observed anisotropy relative to the predicted values.

The results of calculations for acetonitrile and of other nitriles are given in Table 10. It may be noted that the carbon of the cyano group in cyanoacetylene has about the same upfield tensor component as the acetylenic carbons (Table 3). This is quite general and is found with acetonitrile, cyanogen, and dicyanoacetylene (Table 10).

(23) Herzfeld, J.; Berger, A. E. *J. Chem. Phys.* **1980**, *73*, 6021
(24) Pines, A.; Kaplan, S.; Griffin, R. G.; Waugh, J. S. *Chem. Phys. Lett.* **1974**, *25*, 78.
(25) The data were taken from Duncan, T. M. *Principal Components of Chemical Shift Tensors*, 2nd ed.; Farragut Press: Madison, WI, 1997.
(26) Zilm, K. W.; Grant, D. M. *J. Am. Chem. Soc.* **1981**, *103*, 2913.

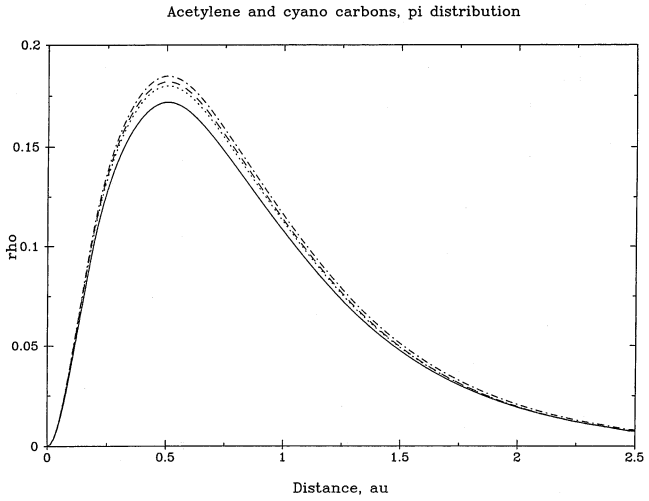

FIGURE 17. Radial distribution of π-electron density at acetylenic and cyano carbons. The circles represent the acetylenic carbons of dicyanoacetylene, the triangles represent the cyano carbons of this compound, and the crosses represent the cyano carbons of cyanogens.

The similarity in chemical shift components suggests that there is little difference in the π-electron density distribution about the acetylenic and cyano carbons. The radial distribution of the electron density at each carbon normal to the bond was calculated and is shown in Figure 17. In accord with expectation, there is essentially no difference between the cyano and acetylenic carbons in their π-electron distributions in the vicinity of the carbons.

9. Conclusions

It is possible to gain additional information about ^{13}C NMR chemical shifts by calculating the tensor components on an MO basis and by examining the matrix elements for the coupling of the occupied orbitals with the virtual orbitals via the angular momentum operator. In the cases of propiolaldehyde and vinylacetylene, the difference in the substituent effects on the long axis (z) tensor components involved occupied orbital MO13 and arose from the location of the nodes in the virtual orbital (MO15) that gave the largest interaction with MO13. This seems to be the primary origin of the β-substituent effect in acetylenes, wherein the acetylenic carbon β to the substituent experiences a much greater change in shielding than the substituted carbon itself. A compensating change in the x and y tensor components for the acetylenic aldehyde was found to arise from a paramagnetic term derived from MO14. A similar analysis for fluoroacetylene provided an explanation for the increased shielding at the unsubstituted carbon as compared to acetylene. The calculated tensor components of the shielding for trimethylsilylacetylene, methoxyacetylene, propiolaldehyde, and acetonitrile are in satisfactory agreement with the experimental data that are presented herein.

10. Experimental Section

Materials. Trimethylsilylacetylene and acetonitrile were commercial samples. Propiolaldehyde was prepared by the chromic acid oxidation of propargyl alcohol,[28] and methoxyacetylene was prepared by the reaction of chloroacetaldehyde dimethylacetal with sodium amide.[29] The identity and purity of all samples were verified using ^{1}H and ^{13}C NMR.

Solid-State Spectra. The ^{13}C NMR static powder spectra for the above compounds were obtained at 7.1 T using a 5 mm VT-MAS probe. Cross-polarization and high-power proton decoupling were employed in all spectra with 3−5 ms contact times. An external sample of adamantane was used as the reference.

To obtain the isotropic chemical shifts in the solid state, the spinning-sideband spectra were obtained by spinning the sample at two different speeds at the magic angle. The isotropic peaks were identified as those whose resonance frequencies are invariant with respect to the spinning speed.

Calculations. The ab initio calculations were carried out using Gaussian 95.[16] The standard program was modified to give the IGAIM shielding terms on an MO basis along with the total shielding and the coupling terms between the occupied and virtual orbitals.[5]

Acknowledgment. This investigation was supported by a grant from the Petroleum Research Fund. J.C.D. acknowledges support via a PRF Type "G" Summer Research Fellowship.

Supporting Information Available: Table of MP2 calculated geometries for the acetylenes. This material is available free of charge via the Internet at http://pubs.acs.org.

JO030258I

(27) Costain, C. C. *J. Chem. Phys.* **1968**, *29*, 864.
(28) Sauer, J. C. *Org. Synth.* **1960** *36*, 66.
(29) Jones, E. R. H.; Eglinton, G.; Whiting, M. C.; Shaw, B. L. *Organic Syntheses*; Wiley: New York, 1963; Collect. Vol. IV, p 404.